

MUTUAL INDUCTANCE MODEL OF THE MECHANICAL STRESS SENSITIVITY OF A POWER TRANSFORMER'S FUNCTIONAL PARAMETERS

Submitted: 21st May 2024; accepted: 26th September 2024

Paweł Rękas, Roman Szewczyk, Tadeusz Szumiata, Michał Nowicki

DOI: 10.14313/JAMRIS/4-2024/28

Abstract:

The mutual inductance model enables testing of the behavior of power transformers under different operation conditions, especially under the environmental influences on the transformer's core. This paper presents the results of an investigation of the stress dependence of the magnetic relative permeability of a power transformer. It was observed that under tensile mechanical stresses up to 98 MPa applied to the core, the transformer input current amplitude increases by almost 67%, whereas the transformer's reactive power increases by 53%. In industrial systems, such changes can potentially lead to unwanted power system shutdowns due to overloading. This effect should be considered during the development of critical power systems.

Keywords: *mutual inductance model, magnetoelastic effect, electric steel*

1. Introduction

Specialized power supplies often operate within their design constraints, where even minor changes can significantly affect performance and safety [1], including the risk of overheating [2, 3]. Understanding these limitations is crucial for ensuring reliability and performance in demanding applications, such as the military [4], aerospace [5], and automotive sectors [6].

The mechanical stress dependence of the magnetic functional characteristics of electric steel sheets has been widely tested, both for non-oriented [7, 8] and grain-oriented electric steels [9, 10]. This paper presents a technical-oriented approach and examines the impact of changes in the magnetic permeability of transformer cores subjected to mechanical stress on their functional performance. The study utilized a specially designed experimental setup [11] to investigate how mechanical stress affects the magnetic permeability of a transformer core. The hypothesis posits that variations in the core's magnetic permeability result in a proportional decrease in inductance, a critical parameter for transformer functionality.

The findings of this research are particularly relevant for designers of the transformers used in high-overload applications where mechanical and thermal stresses are substantial. Designers must thoroughly assess the impact of mechanical stress on transformer performance to prevent potential failures.

Additionally, attention must be paid to heat dissipation during installation to mitigate the effects of stress-induced changes. This consideration is critical in specialized installations, such as aerospace and military applications, where overloads can reach extreme levels.

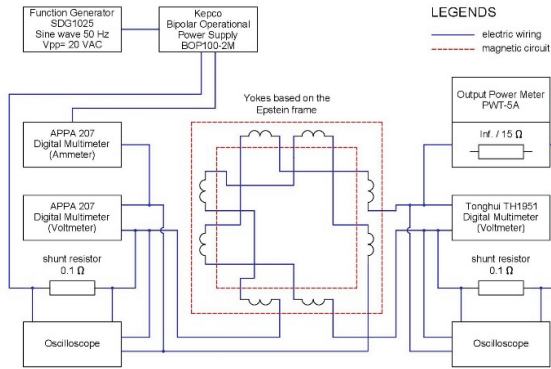
The article focuses on studying the impact of mechanical stress on the functional parameters of a power transformer. In the initial stage, experiments were conducted using three measurement yokes based on the Epstein frame, with frames made of sheet metal cut at different angles relative to the strip axis and the rolling direction. This research aimed to verify the accuracy of the transformer model selection implemented in Matlab Simulink. In the subsequent part of the article, the effect of mechanical stress on the magnetic permeability of M120-27s steel was analyzed. The results were used to assess changes in the permeability of the core of the simulated transformer under mechanical stress. The parameters of a sample single-phase transformer were adopted as the initial values, reflecting the unstressed condition. The transformer model from the Matlab Simulink package, which was selected as the basis for the simulation, met the assumptions verified by Epstein yoke-based measurements regarding the constancy of voltage in the secondary winding and the increase in current in the primary winding with changing inductances of the primary and secondary windings. In the final phase of the study, the impact of mechanical stress on the parameters of the simulated power transformer was determined.

2. Initial Testing of the Model Using Data Obtained From Yokes Based on the Rescaled Epstein Frame with Non-stressed Materials

To validate the assumptions regarding the transformer's response to changes in the magnetic parameters of the transformer core, tests were conducted using measurement yokes based on the rescaled Epstein frame [12, 13]. Three measurement yokes were employed, utilizing strips of transformer sheet metal cut at 0°, 55°, and 90° angles relative to the axis of the sheet strip (magnetization direction) and the rolling direction. The measurement system was configured according to the schematic shown in Figure 1.

Table 1. Results of the measurement yokes based on the Epstein frame

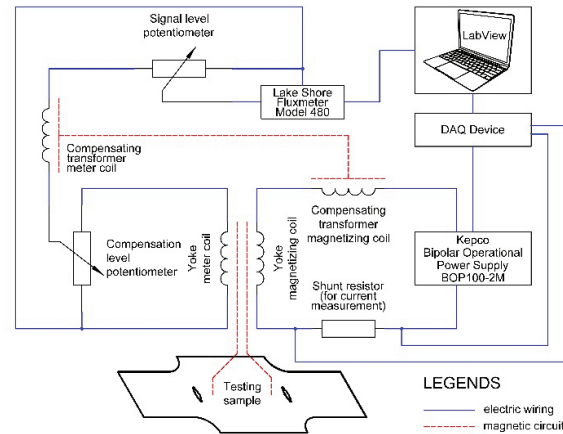
α	L_{Pri} , mH	L_{Sec} , mH	Load, Ω	V_p , V	I_p , A	V_s , V	P_s , W
0°	111.1	108.4	∞	6.51	0.14	6.32	0.0
			15.0	6.49	0.26	3.19	10.5
90°	13.5	12.9	∞	6.50	0.38	6.11	0.0
			15.0	6.48	0.35	3.09	10.0
55°	18.1	17.3	∞	6.44	1.01	5.32	0.0
			15.0	6.44	0.85	2.8	8.25

**Figure 1.** Wiring diagram of the measuring yoke based on the Epstein frame

Initial inductance measurements were taken for both the primary L_{Pri} and secondary L_{Sec} windings of the transformer. The inductances were measured using a Handheld LCR Meter TH2822A, manufactured by Tonghui. The results of the transformer response and initial inductance measurements are presented in Table 1.

The experimental setup began with a function generator producing a sinusoidal waveform at 50 Hz with a peak-to-peak voltage (V_{pp}) of 20 VAC. This signal was amplified using a Kepco BOP100-2M amplifier. The amplified signal passed through an ammeter (Appa 207) and a 0.1Ω shunt resistor before reaching the magnetizing windings of the measurement yoke. A voltmeter (Appa 207) was connected in parallel with the magnetizing winding to measure the voltage. An oscilloscope monitored the voltage across the shunt resistor and the magnetizing winding.

The measurement winding of the yoke was tested under two conditions: no load condition, where the winding was not connected to any external load, and loaded condition, where an output power meter (PWT-5A) was connected with a load set at 15Ω . The 15Ω load was selected, under which the most significant power output was observed from the measurement winding. The measurement winding was connected to this load through an ammeter (Appa 207) and a 0.1Ω shunt resistor. A voltmeter (Tonghui TH1951) measured the voltage across the measurement winding, while the oscilloscope captured both the voltage across the shunt resistor and the measurement winding voltage.

**Figure 2.** Wiring diagram of the measurement setup

Data collected included power meter readings from the measurement winding, voltage across the magnetizing winding, current through the magnetizing winding, and voltage across the measurement winding. These values are summarized in Table 1, demonstrating the impact of core magnetic permeability on the transformer's electrical parameters.

The results unequivocally indicate that as the magnetic permeability of the core material decreases, the voltage and power on the secondary winding of the transformer remain largely unchanged within the tested range. However, a significant increase in the current on the primary winding is observed.

3. The Method of Measuring Stress Dependence of 2D Magnetization Characteristics in Electrical Steel Sheets

A specialized measurement setup based on a magnetic yoke was developed to investigate the effect of the mechanical stress dependence on the magnetic properties of electrical steels [11]. The mechanical part of the setup was prepared with a focus on the stress application device [14], and a specially designed specimen shape was created to ensure optimal stress distribution [15]. An automatic system for positioning the yoke throughout the testing cycle was also developed. The testing process control system, signal analysis, and data processing system were established. This setup is described in detail in [11]. The wiring diagram is shown in Figure 2.

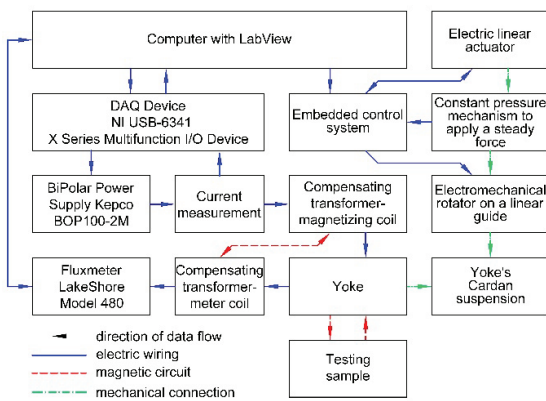


Figure 3. Schematic block diagram of the measurement setup

The information flow diagram is presented in Figure 3. The setup is controlled by a computer equipped with LabView software and a DAQ Device NI USB-6341 data acquisition card. The magnetic flux in the yoke is measured using a LakeShore model 480 fluxmeter. The actuators are managed by an embedded system based on a microcontroller that controls the rotation and linear motion of the yoke system head.

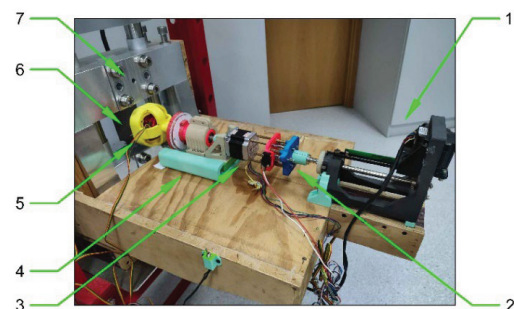
3.1. The Experimental Setup

The developed setup operates automatically and performs a complex series of measurements. By using specimens cut at various angles between the direction of the applied stress (specimen axis) and the rolling direction of the sheet, it is possible to study changes in magnetic permeability as a function of varying stress, the angle between the stress direction and rolling direction, and the angle between the specimen axis and the magnetization direction. Combined with an automatically rotating yoke [11], this facilitates a wide range of possible research.

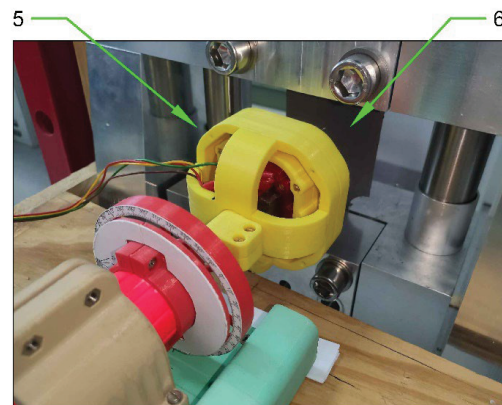
The measurement process, with the experimental setup presented in Figure 4, begins by mounting the specimen in a mechanical module to apply stresses (7). The mechanical module is positioned on a mechanical press, which applies the appropriate stresses to the clamped sample. The yoke system head (5) with the attached measuring yoke is pressed against the sample during the measurement. The force applied remains constant throughout a single cycle due to the use of a linear overload clutch and the locking of the linear actuator in the measuring position. Upon completing the measuring cycle, the yoke system head retracts and performs a controlled rotary motion to the next measuring position using the rotator stepper motor (3). The entire assembly, coupled to the linear actuator, moves along the linear guide (4).



(a)



(b)



(c)

Figure 4. Photography of the measurement setup: (a) tested sheet sample, (b) general view of the measurement system, and (c) measuring head during the measurement process: 1 – linear actuator, 2 – cushioning mechanism, 3 – rotator with stepper motor, 4 – linear rolling guide, 5 – measuring head, 6 – tested sheet sample, 7 – mechanical module for mounting and applying stresses to the tested sample

M120-27s electrical steel [16] sheet samples with a specially designed shape were used for the measurements. The specimen comprises three sections: the first and third sections were used solely for mounting the specimens in the mechanical module and did not participate in the study of magnetic properties, while the second section was subjected to stress, and its magnetic properties were studied. During the test, the measuring yoke is pressed against the measuring section.

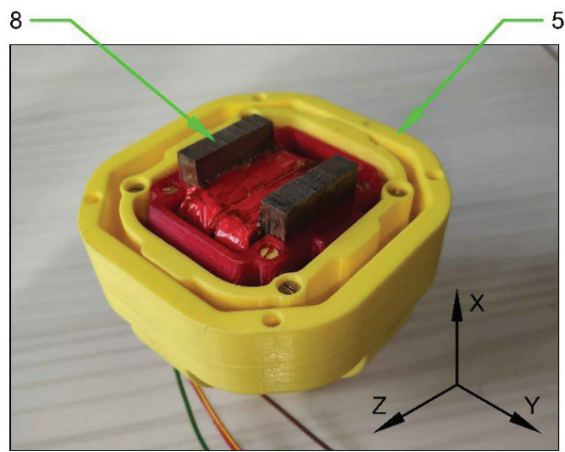


Figure 5. The measuring head (5), made of non-magnetic materials, features a 2D Cardan gyroscope mechanism and a measuring yoke (8)

The specimen's shape is optimized using the finite element method to ensure a uniform stress distribution [11]. The specimens are clamped in a non-magnetic mechanism. Only tensile stresses are applied due to the low force required to buckle the specimens.

3.2. Automatically Adjusting the Yoke System

Magnetic yokes provide the best results when measuring the directional properties of transformer sheets. However, when studying the angular properties of the sheets over a full 360-degree range with high-resolution yoke positioning, the manual operation becomes inefficient due to the lengthy measurement times involved. The solution to this problem is implementing an automatic measurement system based on a mechatronic setup that positions the yoke accurately.

Automated measurements require ensuring that the yoke is pressed against the sample in the most effective and, crucially, repeatable manner. This consistency was achieved by suspending the yoke on a Cardan joint. The developed system allows the yoke to maneuver with four degrees of freedom. The positioning of the yoke itself uses two degrees of freedom: XY and XZ rotation of the yoke in the head. Additionally, the YZ rotation of the entire head and linear movement along the X-axis enable complete 360-degree testing. A photograph of the yoke holder with Cardan suspension and axis description is shown in Figure 5.

3.3. Uncertainty Analysis and Error Mitigation in the Measurement Configuration

The presented test stand was designed to measure relative magnetic permeability, with particular attention to the dependence of this permeability on the angles between the direction of external mechanical stresses, the rolling direction of the transformer sheet, and the direction of magnetization. A detailed description of the uncertainty determination method can be found in [11].

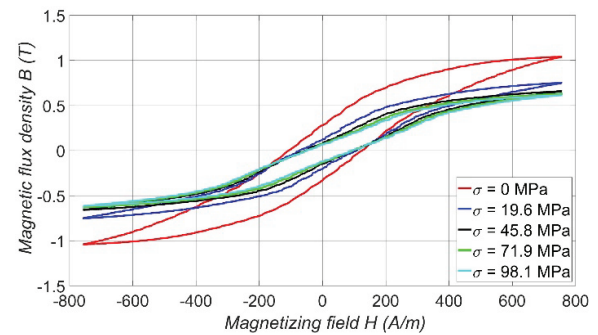


Figure 6. The influence of mechanical tensile stresses σ on the shape of the magnetic hysteresis loop $B(H)$ of M120-27 s grain-oriented electrical steel

The main factor influencing changes in relative permeability (μ_r) was the varying intensity of the magnetizing field. Therefore, the A-type uncertainty, denoted as $u(\mu_r)$, was estimated based on the calculated values of μ_r with a 95% confidence level, depending on the applied magnetizing field strength H . It is worth noting that beyond the initial level of H , where significant interaction between remanent magnetization and demagnetizing fields occurs, the A-type uncertainty of the proposed measurement system does not exceed 0.5%.

With the maximum resolution of positioning the measurement yoke relative to the sample under test—200 positions over the entire 360-degree range—and considering the response to different magnetization fields, measurements can take many hours. Under such conditions, the drift of the LakeShore fluxmeter model 480 can be observed. The drift affecting the measured values was addressed by automatic calibration of the fluxmeter, performed after each yoke rotation.

Mechanical stresses are applied using a hydraulic actuator equipped with a pressure control system, ensuring the stability of the applied mechanical stresses throughout the test.

4. The Results of Experimental Measurements

The effect of mechanical stresses on M120-27s grain-oriented electrical steel was measured, with tensile stresses applied in the rolling direction. The specimen was subjected to five levels of stress: $s_1 = 0$ MPa, $s_2 = 19.6$ MPa, $s_3 = 45.8$ MPa, $s_4 = 71.9$ MPa, $s_5 = 98.1$ MPa. The steel sheet was magnetized with a field strength of 750 A/m in alignment with the rolling direction. The measured hysteresis loops are presented in Figure 6.

The relative magnetic permeability of the sample during each stress was determined using the following relationship:

$$\mu_r = \frac{1}{\mu_0} \cdot \frac{B_{max}}{H_{max}} \quad (1)$$

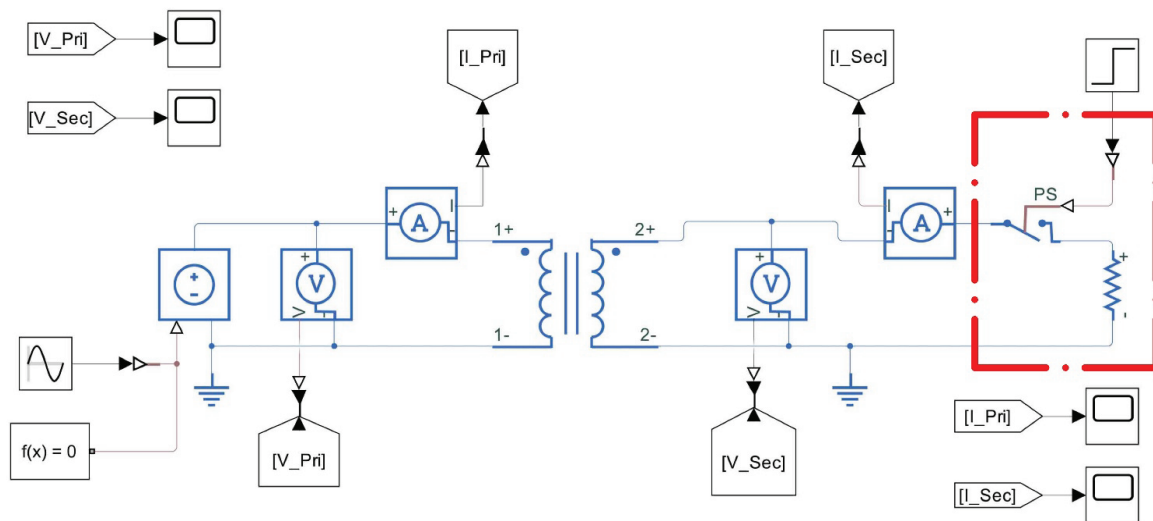


Figure 7. The Matlab Simulink model of the electrical transformer system includes a mutual inductor. The load, which is switched on halfway through the simulation, is highlighted with a red box

It was observed that as the stress applied to the sample increases, the relative magnetic permeability decreases. Since the inductance of transformer windings is partially dependent on the magnetic permeability of the transformer core, it is assumed that a decrease in the magnetic permeability of the stressed transformer core will result in a proportional decrease in the inductance of both the primary and secondary windings.

5. Modeling the Impact of Mechanical Stress on the Functional Parameters of Power Transformers

To investigate the impact of mechanical stress on the functional parameters of power transformers, the Mutual Inductor model from the Simscape library was used. The model is governed by the following equations [17]:

$$V_1 = L_1 \frac{dI_1}{dt} + M \frac{dI_2}{dt} \quad (2)$$

$$V_2 = L_2 \frac{dI_2}{dt} + M \frac{dI_1}{dt} \quad (3)$$

$$M = k \sqrt{L_1 \cdot L_2} \quad (4)$$

V_1 represents the induced voltage across the primary winding, while V_2 is the induced voltage across the secondary winding. I_1 is the current entering the positive terminal of the primary winding, and I_2 is the current leaving the positive terminal of the secondary winding. L_1 and L_2 are the self-inductances of the windings, M is the mutual inductance, k is the coupling coefficient, and t is time.

Other transformer models available in Simscape [18] were also evaluated, but none yielded satisfactory results consistent with the validated data. The final configuration of the model used for the simulations is depicted in Figure 7.

The voltage V_1 on the primary winding was set to 230 VAC RMS at 50 Hz. Initially, the voltage V_2 on the secondary winding was a no-load voltage from the start to the midpoint ($t = 0.25$ s) of the simulation. From the midpoint to the end of the simulation, the secondary winding was automatically loaded with a resistor of $R = 8 \Omega$. For the purposes of the simulation, the coefficient of coupling, which determines the mutual inductance M , was assumed to be $k = 0.9$. Simulations were conducted in the time domain t , with a total simulation time of 0.5 seconds. The figures illustrate the period from $t_1 = 0.2$ s to $t_2 = 0.3$ s.

The initial parameters for the model were derived from a real transformer, model TE-4812167, manufactured by Hua Jia Electric Appliance Co., Ltd. The transformer operates with a primary winding voltage of 230–240 V at 50 Hz, a secondary winding voltage of 12 V, and a maximum current of 1.67 A. The power rating of the transformer is 20 VA. The inductances were measured using a Handheld LCR Meter, model TH2822A, manufactured by Tonghui. The inductance L_{Pri} of the primary winding was measured to be 11.836 H, and the inductance L_{Sec} of the secondary winding was 35.323 mH. Based on these values and the reduction in magnetic permeability of the transformer sheet under mechanical stress, the decrease in inductance of both the primary and secondary windings of the simulated transformer was calculated. It was assumed that there is a linear relationship between stress and magnetic permeability in the initial ranges of mechanical stress. However, for higher stress values, this relationship becomes nonlinear. The values used in the simulation are presented in Table 2.

In order to thoroughly analyze and investigate the impact of mechanical stress on the functional parameters of power transformers, the active power P and reactive power Q were calculated. These values were obtained using a dedicated Simulink block.

Table 2. Inductances L_{Pri} and L_{Sec} of transformer windings as a function of simulated tensile stresses applied to the transformer core

σ , MPa	L_{Pri} , H	L_{Sec} , uH
0	11.836	35.323
19.6	8.542	25.492
45.8	7.489	22.350
71.9	7.157	21.358
98.1	7.027	20.971

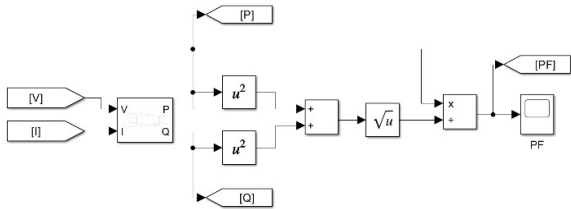


Figure 8. The model of an electrical transformer system in Matlab Simulink—the section of the model responsible for calculating active power P, reactive power Q, and power factor PF

Table 3. Measured current amplitude (I) in the primary winding

σ , MPa	Amplitude	
	I_{Pri} at t_1	I_{Pri} at t_2
0	0.088	0.127
19.6	0.121	0.150
45.8	0.138	0.163
71.9	0.144	0.168
98.1	0.147	0.170

The power factor PF was calculated as the ratio of real power to apparent power in a given moment, as shown in Equation (5).

$$PF = \frac{P}{S} \tag{5}$$

The complex power S was determined as the vector sum of active and reactive power, expressed as:

$$S^2 = P^2 + Q^2 \tag{6}$$

The section of the model responsible for calculating power is depicted in Figure 8.

6. Results of Simulation Studies on Mechanical Stress Effects in Power Transformers

Simulations were performed for 5 different stresses. The results of the simulations are shown in Figures 9, 10, and 11 and summarized in Tables 3–7.

Table 3 shows the current amplitude in the primary winding of the transformer for different levels of stress σ expressed in MPa, measured at two moments in time, t_1 and t_2 . Increasing the stress causes an increase in the amplitude of the current in the primary winding. The most significant increase in current amplitude is observed when the tension rises from 0 to 19.6 MPa.

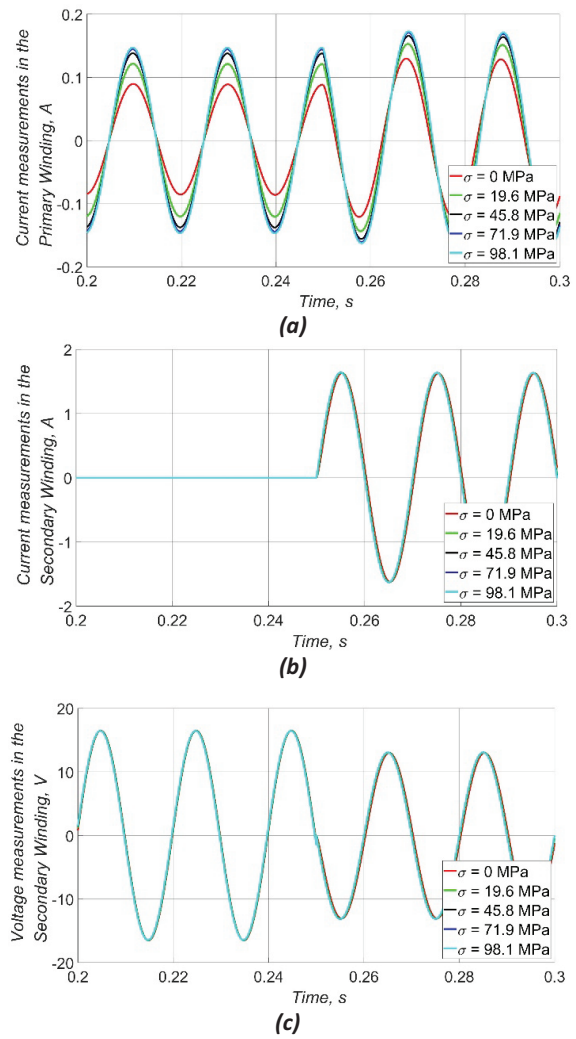


Figure 9. Results of the simulations—oscillograms of current and voltage on the windings of the simulated transformer: (a) measured current in the primary winding as a function of time, (b) measured current in the secondary winding as a function of time, and (c) measured voltage in the secondary winding as a function of time

Table 4. Measured active power (P) in the primary winding

σ , MPa	Amplitude		Average value	
	P_{Pri} at t_1	P_{Pri} at t_2	P_{Pri} at t_1	P_{Pri} at t_2
0	2.379	3.427	0.728	13.059
19.6	3.270	4.063	1.384	13.754
45.8	3.721	4.413	1.795	14.140
71.9	3.890	4.549	1.963	14.294
98.1	3.961	4.606	2.035	14.360

Table 4 presents the amplitude and average value of active power in the primary winding of the transformer at different stress levels, measured at two moments in time. The amplitude and the average value of active power increase with increasing stress.

Table 5 shows the amplitude and average value of active power in the secondary winding of the transformer for different stress levels.

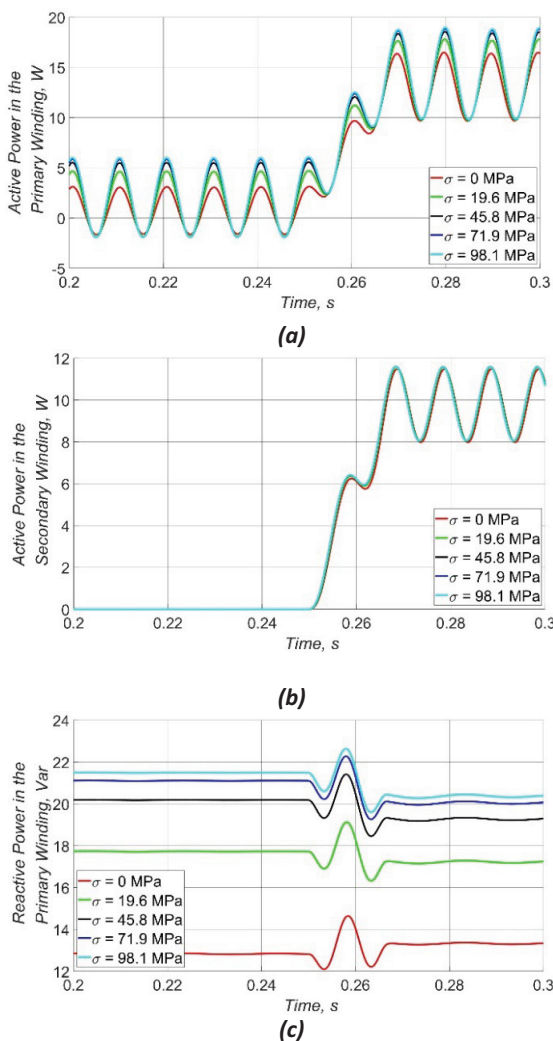


Figure 10. Results of the simulations—oscillograms of power on the windings of the tested transformer: (a) active power P in the primary winding, (b) active power P in the secondary winding, and (c) reactive power Q in the primary winding

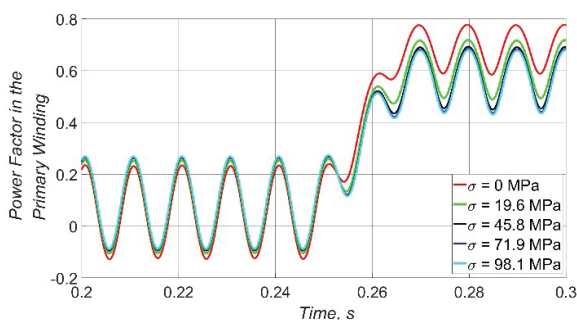


Figure 11. Results of the simulations—power factor PF oscillogram in the primary winding

The amplitude of active power in the secondary winding is relatively stable, suggesting that changes in stress have less effect on this winding. The average active power values are almost constant regardless of the stress level, which may indicate the transformer's efficiency in maintaining power in the secondary circuit.

Table 5. Measured active power (P) in the secondary winding

σ , MPa	Average value	
	P_{Pri} at t_2	P_{Pri} at t_1
0	1.756	9.727
19.6	1.771	9.806
45.8	1.773	9.817
71.9	1.774	9.818
98.1	1.774	9.818

Table 6. Measured reactive power (Q) in the primary winding

σ , MPa	Average value	
	Q_{Pri} at t_1	Q_{Pri} at t_2
0	12.824	13.319
19.6	17.722	17.216
45.8	20.179	19.259
71.9	21.100	20.034
98.1	21.484	20.359

Table 7. Measured power factor (PF) in the primary winding

σ , MPa	Amplitude		Average value	
	PF_{Pri} at t_1	PF_{Pri} at t_2	PF_{Pri} at t_1	PF_{Pri} at t_2
0	0.181	0.096	0.0538	0.681
19.6	0.180	0.115	0.0741	0.604
45.8	0.179	0.122	0.0843	0.571
71.9	0.179	0.124	0.0882	0.560
98.1	0.179	0.125	0.0898	0.556

Table 6 illustrates the average values of reactive power in the primary winding of the transformer at different stress levels. Reactive power increases as stress increases, suggesting more significant inefficiency at higher stress levels. Reactive power values are highest for the most critical stresses, which may require compensation to improve transformer efficiency or overload reactive power compensation systems for systems that do not anticipate reactive power increasing with core stress.

Table 7 presents the amplitude and average value of the power factor in the primary winding for different stress levels. The power factor tends to decrease with increasing stress, indicating a decrease in power efficiency. The need to improve the power factor may require additional measures, such as the use of reactive power compensation.

7. Conclusion

Applying mechanical stress to the transformer core significantly changes its electrical parameters. It is worth noting that within the tested ranges, the output parameters, such as current and voltage, remain largely unchanged. However, significant changes occur in the primary winding, where the current amplitude increases by almost 67% under extreme stress conditions. These are critical changes, as they have a profound effect on the key operational parameters of the transformer.

This phenomenon can be extremely dangerous because these changes are not detectable on the load side of the transformer. The changes in operating parameters also affect the power system, as the transformer's reactive power is seen to increase by almost 53% when operating under load, potentially leading to unwanted power system shutdowns due to overloading.

It should be highlighted that a quantitative description of the influence of mechanical stresses on the functional properties of the power transformer plays a vital role in both the efficient development of the power transformer system as well as during its safe exploitation. On the basis of the proposed quantitative model and the proposed method of experimental measurements of the stress-dependence of 2D relative magnetic permeability, it is possible to predict the operating conditions and properly select the magnetic material for the core of the power transformer.

The simulation results were compared with measurements of the material's properties and its effect on the transformer. However, full validation of the impact of stress on the transformer requires the preparation of a test stand under natural conditions that accurately reflect the device's actual operating conditions.

AUTHORS

Paweł Rękas – Faculty of Mechatronics, Warsaw University of Technology, Poland, e-mail: pawel.rekas.dokt@pw.edu.pl.

Roman Szewczyk* – Łukasiewicz Research Network – Industrial Research Institute for Automation and Measurements PIAP, Poland, e-mail: roman.szewczyk@pw.edu.pl.

Tadeusz Szumiata – Faculty of Mechanical Engineering, Department of Physics, Kazimierz Pulaski Radom University, Poland, e-mail: t.szumiata@uthrad.pl.

Michał Nowicki – Department of Mechatronics, Robotics and Digital Manufacturing, Faculty of Mechanics, Vilnius Gediminas Technical University, Lithuania, e-mail: michal.nowicki@pw.edu.pl.

*Corresponding author

References

- [1] L. Cesky, F. Janicek, and J. Kubica et al., "Overheating of Primary and Secondary Coils of Voltage Instrument Transformers," *2017 18th International Scientific Conference on Electric Power Engineering (EPE)*, May 2017. doi: 10.1109/ep.e.2017.7967359.
- [2] K. Liu, "Intelligent Identification Method of Transformer Overheat Fault in Distribution Substation Based on Deep Learning Algorithm and Infrared Temperature Measurement Technology," *2023 3rd International Conference on Electrical Engineering and Control Science (IC2ECS)*, Dec. 2023. doi: 10.1109/ic2ecs60824.2023.10493404.
- [3] K. S. Kassi, I. Fofana, and F. Meghnefi et al., "Impact of Local Overheating on Conventional and Hybrid Insulations for Power Transformers," *IEEE Transactions on Dielectrics and Electrical Insulation*, vol. 22, no. 5, pp. 2543–2553, Oct. 2015. doi: 10.1109/tdei.2015.005065.
- [4] C. Qingsong et al., "Analysis of Transformer Abnormal Heating Based on Infrared Thermal Imaging Technology," *2018 2nd IEEE Conference on Energy Internet and Energy System Integration (EI2)*, Oct. 2018. doi: 10.1109/ei2.2018.8582496.
- [5] K. Furmanczyk and M. Stefanich, "Overview of Multiphase Power Converters for Aerospace Applications," *SAE Technical Paper Series*, Nov. 2008. doi: 10.4271/2008-01-2878.
- [6] M. Yamamoto, T. Kakisaka, and J. Imaoka, "Technical Trend of Power Electronics Systems for Automotive Applications," *Japanese Journal of Applied Physics*, vol. 59, no. SG, Apr. 2020. doi: 10.35848/1347-4065/ab75b9.
- [7] N. Leuning, S. Steentjes, and K. Hameyer, "Effect of Magnetic Anisotropy on Villari Effect in Non-oriented FESI Electrical Steel," *International Journal of Applied Electromagnetics and Mechanics*, vol. 55, pp. 23–31, Oct. 2017. doi: 10.3233/jae-172254.
- [8] M. Yamagashira, S. Ueno, and D. Wakabayashi et al., "Vector Magnetic Properties and Two-Dimensional Magnetostriction of Various Soft Magnetic Materials," *International Journal of Applied Electromagnetics and Mechanics*, vol. 44, nos. 3–4, pp. 387–400, Mar. 2014. doi: 10.3233/jae-141801.
- [9] E. Beyer, L. Lahn, and C. Schepers et al., "The Influence of Compressive Stress Applied by Hard Coatings on the Power Loss of Grain Oriented Electrical Steel Sheet," *Journal of Magnetism and Magnetic Materials*, vol. 323, no. 15, pp. 1985–1991, Aug. 2011. doi: 10.1016/j.jmmm.2011.02.044.
- [10] K. Fonteyn, A. Belahcen, and A. Arkkio, "Properties of Electrical Steel Sheets under Strong Mechanical Stress," *Pollack Periodica*, vol. 1, no. 1, pp. 93–104, Apr. 2006. doi: 10.1556/pollack.1.2006.1.7.
- [11] P. Rękas et al., "A Measuring Setup for Testing the Mechanical Stress Dependence of Magnetic Properties of Electrical Steels," *Journal of Magnetism and Magnetic Materials*, vol. 577, p. 170791, Jul. 2023. doi: 10.1016/j.jmmm.2023.170791.
- [12] P. Marketos, S. Zurek, and A. J. Moses, "A Method for Defining the Mean Path Length of the Epstein Frame," *IEEE Transactions on Magnetics*, vol. 43, no. 6, pp. 2755–2757, Jun. 2007. doi: 10.1109/tmag.2007.894124.
- [13] D.-X. Chen and Y.-H. Zhu, "Effective Magnetic Path Length in Epstein Frame Test of Electrical Steels,"

- Review of Scientific Instruments*, vol. 93, no. 5, May 2022. doi: 10.1063/5.0084859.
- [14] P. Rekas, T. Szumiata, and R. Szewczyk et al., "Influence of Mechanical Stresses Noncoaxial with the Magnetizing Field on the Relative Magnetic Permeability of Electrical Steel," *IEEE Transactions on Magnetics*, vol. 60, no. 8, pp. 1–9, Aug. 2024. doi: 10.1109/tmag.2024.3418668.
- [15] T. Szumiata, P. Rekas, and M. Gzik-Szumiata et al., "The Two-Domain Model Utilizing the Effective Pinning Energy for Modeling the Strain-Dependent Magnetic Permeability in Anisotropic Grain-Oriented Electrical Steels," *Materials*, vol. 17, no. 2, p. 369, Jan. 2024. doi: 10.3390/ma17020369.
- [16] EN 10107:2022 Grain-Oriented Electrical Steel Sheet and Strip Delivered in the Fully Processed State. doi: 10.3403/30092684.
- [17] "Mutual Inductor," *Mutual Inductor in Electrical Systems – MATLAB*, <https://www.mathworks.com/help/simscape/ref/mutualinductor.html> (accessed Aug. 11, 2024).
- [18] "Simscape Electrical," *Simscape Electrical Documentation*, <https://www.mathworks.com/help/sps/index.html> (accessed Aug. 11, 2024).